Overexpression of GPER1 suppressed esophageal carcinoma growth *via* activating cAMP pathway

Hongmei Yin,[1,2] Xiumei Han,[2] Qun Zhang,[2] Duojie Li,[2] Fan Wang[1]

[1]Department of Radiation Oncology, The First Affiliated Hospital of Anhui Medical University, Hefei
[2]Department of Radiotherapy, The First Affiliated Hospital of Bengbu Medical University, Bengbu, China

ABSTRACT

G protein-coupled estrogen receptor 1 (GPER1) has extensively verified as a tumor regulator in various types of cancers. However, its role in esophageal cancer (EC) remains largely unclear. In this study, the expression and prognostic prediction value of GPER1 in EC was analyzed by using TCGA database and was verified in EC cells and fresh tissues. The results showed that GPER1 is decreased in EC cells and tissues, and lower GPER1 expression is associated with poor overall survival of EC patients. CCK-8 assay and flow apoptosis cytometry were applied to measure the ability of proliferation and apoptosis of EC cells with or without GPER1 overexpression. The levels of reactive oxygen species (ROS) and Fe^{2+} were determined by flow cytometry. Elisa and Western blotting were employed to measure the markers of ferroptosis and cyclic adenosine monophosphate (cAMP) pathway. The results of *in vitro* experiments indicated that overexpression of GPER1 caused decreased proliferation, increased cell apoptosis, ROS generation, Fe^{2+} content and acyl-CoA synthetase long-chain family member 4 (ACSL4) expression, while decreased glutathione peroxidase 4 (GPX4) expression. Notably, the cAMP/PKA inhibitor H89 significantly reversed the ferroptotic effects induced by GPER1, indicating the essential role of the cAMP pathway in this process. The weight and volumes of tumors were measured and Ki-67 and H&E staining were conducted to analyze the effect of GPER1 *in vivo*. The results of *in vivo* experiments indicated that overexpression of GPER1 resulted in restricted tumor growth, reduced Ki-67 expression and increased cell death. In conclusion, the expression of GPER1 is reduced in EC. Overexpression of GPER1 enhances ferroptosis in EC, primarily through activation of the cAMP signaling pathway.

Key words: G protein-coupled estrogen receptor 1; ferroptosis; esophageal carcinoma; GPX4.

Correspondence: Fan Wang, Department of Radiotherapy, The First Affiliated Hospital of Anhui Medical University, No. 218 Jixi Road, Hefei 233000, Anhui, China. E-mail: wangfan6682024@163.com

Contributions: Hongmei Yin, data analysis and interpretation, histological examination, writing- original draft preparation. Xiumei Han, Qun Zhang, Duojie Li, data analysis and interpretation. Fan Wang, histological examination, writing- original draft preparation. All authors read and approved the final version of the manuscript and agreed to be accountable for all aspects of the work.

Conflict of interest: the authors declare no competing interests and all authors confirm accuracy.

Ethics approval: this study was approved by the Clinical Research Ethics Committee of Bengbu Medical University (approval No. 2025-(Lunshen)-541). Informed consent was obtained from all participants. All animal experiments were approved by the Animal Ethics Committee of Bengbu Medical University (approval No. 2025-(Lunshen)-730) and were carried out in accordance with relevant guidelines and regulations.

Availability of data and materials: all data is available upon reasonable request from the corresponding author.

Funding: this work was supported by the Natural Science General Program of Bengbu Medical University (No. 2024byzd061) and the Research Funds of Joint Research Center for Regional Diseases of IHM (No. 2024bydjk009).

Introduction

Esophageal cancer (EC) ranks as the eighth most prevalent cancer and the sixth leading cause of cancer-related mortality globally.[1,2] Annually, approximately 450,000 individuals are diagnosed with EC, and over 400,000 succumb to the disease worldwide.[2] Surgical resection remains the sole curative treatment for EC; however, it is not feasible for 50-60% of patients.[3,4] For these individuals, palliative treatment modalities, including stent placement, intracavitary brachytherapy, external beam radiotherapy, laser therapy, photodynamic therapy, and chemotherapy, are the primary therapeutic options.[2,5] Despite ongoing advancements in palliative care, the 5-year survival rate for patients with advanced EC remains dismally low, at 20-25%.[6] Recently, molecular targeted therapies have shown promising potential in the management of EC. However, the limited availability of therapeutic targets and the emergence of drug resistance pose significant challenges to their clinical application. Consequently, there is a critical need to identify novel targets and address drug resistance to enhance the efficacy of molecular targeted therapies. Ferroptosis, a term introduced by Dixon *et al*. in 2012, refers to a distinct mode of cell death.[7] The fundamental characteristic of ferroptosis involves the depletion of glutathione (GSH) and the consequent reduction in the activity of GPX4, leading to the accumulation of lipid peroxides and the generation of ROS.[8] This form of cell death is markedly different from necrosis, apoptosis, and autophagy, primarily characterized by pronounced mitochondrial shrinkage, increased membrane density, and the reduction or disappearance of mitochondrial cristae.[9,10] Inducing ferroptosis has the potential to overcome drug resistance and induce cell death, making it a promising target for cancer therapy.[11,12] However, in the context of EC, the regulatory mechanisms that protect EC cells from ferroptosis remain largely undefined. G protein-coupled estrogen receptor 1 (GPER1, also known as GPR30) is a prototypical G protein-coupled receptor encoded by the GPER1 gene, which is situated on chromosome 7. GPER1 is predominantly localized to the membranes of the endoplasmic reticulum and the Golgi apparatus.[13] GPER1 comprises seven transmembrane α-helices, along with four intracellular and four extracellular loops.[14] The extracellular loops are primarily responsible for ligand recognition and binding, while the intracellular segments facilitate binding to G proteins, thereby initiating intracellular signal transduction pathways.[15-17] GPER1 demonstrates tissue-specific functions, exhibiting both tumor-promoting and tumor-suppressing activities. Specifically, GPER1 has been shown to exert anti-tumor effects in gastric, ovarian, and liver cancers,[18-20] whereas it functions as an oncogene in lung, prostate, cervical, glioblastoma, and breast cancers.[21,22] To sum up, the function of GPER1 is tissue-specific, which can promote or inhibit the malignant phenotype of various cancers, but its role in EC is largely unclear. In this study, we initially investigated the expression levels of GPER1 in EC and observed a reduction in its expression. Subsequently, we conducted both *in vivo* and *in vitro* experiments to assess the functional role of GPER1, discovering its protective effect on EC through mechanisms involving ferroptosis. Lastly, we examined the underlying mechanism by which GPER1 inhibits ferroptosis.

Materials and Methods

Tissue samples

Six paired EC samples and para-tumor samples were collected from First Affiliated Hospital of Bengbu Medical University from January 2014 to September 2015. The ethics related documents involved in this project were approved by Ethics Committee of Bengbu Medical University (2025-(Lunshen)-541) and all the six enrolled patients signed the consent form.

Cell lines

Normal human esophageal epithelial cell line (HEEC) and EC cell lines (EC9706, TE-1, KYSE150, KYSE70, ECA-109 and KYSE30) were obtained from the FuHeng biology Co., Ltd. (Shanghai, China). HEEC cells were cultured in Dulbecco's Modified Eagle Medium (DMEM; Gibco, Waltham, MA, USA). All EC cell lines were cultured in RPMI 1640 medium (Gibco) 10% fetal bovine serum (FBS). All applied cell lines contained complete short tandem repeats (STR) reports.

Construction of GPER1 overexpression and knockdown EC cell lines

The plasmid targeted GPER1 was constructed by Vigen Biotechnology Co., Ltd. (Jiangsu, China) to overexpressed GPER1 (GPER1-OE) in KYSE70 and KYSE150, and EC9706 cell lines. The plasmid contained the full-length human GPER1 coding sequence (CDS) driven by a CMV promoter, along with a puromycin resistance gene for selection. For the knockdown experiment, small interfering RNA (siRNA) targeting GPER1 (si-GPER1) and negative control siRNA (si-NC) were designed and synthesized by the same company. The sequence for si-GPER1 was 5'-GCA ACA GCA UCA ACG UCA ATT-3', and the negative control siRNA (si-NC) sequence was 5'-UUC UCC GAA CGU GUC ACG UTT-3'. For lentiviral transduction, KYSE70, KYSE150, and EC9706 cells were infected with the GPER1 overexpression lentivirus or a negative control (NC) lentivirus. Stably transfected cell pools were selected and maintained using 2 μg/mL puromycin for at least two weeks. KYSE150 cells were transfected with si-GPER1 or si-NC using Lipofectamine 3000 (Invitrogen, Carlsbad, CA, USA) according to the manufacturer's instructions and harvested for experiments 48-72 h post-transfection. Quantitative real-time PCR (qRT-PCR) and Western bolt were employed to measure the efficiency of transduction and transfection.

Construction of EC mice model

Female BALB/C nude mice (5 weeks old) were purchased from the Nanjing Institute of Model Biology and housed under specific pathogen-free (SPF) conditions. To establish the xenograft model, KYSE70 cells stably transfected with negative control (NC) or GPER1-overexpressing (GPER1-OE) lentivirus were harvested and resuspended in sterile PBS. A total of 5×10^6 cells in 100 μL PBS were subcutaneously injected into the right flank of each mouse. The mice were randomly divided into two groups (n=5 per group): the NC group and the GPER1-OE group.

Tumor formation was monitored regularly, and tumor volumes were measured every 3-4 days using a caliper and calculated with the formula: volume = (length × width^2)/2. At the end of the experiment (day 32), all mice were anesthetized by intraperitoneal injection of 0.1 mL of 1% phenobarbital sodium. Tumors were excised, photographed, and weighed. All procedures involving animals were conducted in accordance with the Guide for the Care and Use of Laboratory Animals (National Institutes of Health, Bethesda, MD, USA) and were approved by the Institutional Animal Care and Use Committee of Anhui Medical University (Approval No. 2025-(Lunshen)-730).

RNA extraction and qRT-PCR

Total RNA was isolated from EC cells using AG RNAex Pro

RNA Kit (Accurate Biotechnology, Zhejiang, China) and then was converted to cDNA with Evo M-MLV RT Master Mix (Accurate Biotechnology). The qRT-PCR was finally conducted through SYBR Green Pro Taq HS Premix (Accurate Biotechnology). The expression of GPER1 was analyzed based on $2^{-\Delta\Delta Ct}$ method and GAPDH was used as endogenous reference. All experiments were conducted according to the manufacturer's protocol provided. The applied sequences of the primers for GPER1 were 5'-CACCAGCAGTACGTGATCG G-3' (forward) and 5'-CATCTTCTCGCGGAAGCTGAT-3' (reverse). The applied sequences of the primers for GAPDH were 5'-GGAGCGAGATC-CCTCCAAAAT-3' (forward) and 5'-GGCTGTTGTCAT-ACTTCTCATGG-3' (reverse).

Protein extraction and Western blot

Total protein was obtained from EC cells by radio immunoprecipitation assay lysis buffer (RIPA; Solarbio, Beijing, China) and subsequently quantified by bicinchoninic acid (BCA) Kit (Beyotime Biotechnology, Shanghai, China). Then, the protein was boiled at 95°C for 5 min. After that, the boiled protein was loaded into sodium dodecyl sulfate-polyacrylamide gel electrophoresis (SDS-PAGE) gel and was then transferred onto polyvinylidene fluoride membranes (PVDF; MilliporeSigma, Burlington, MA, USA). Moreover, the PVDF membranes were incubated with primary antibodies overnight at 4°C, and then was incubated with secondary antibodies for 1 h at room temperature. The primary antibodies were anti-GPER1 (ABclonal Technology, Zhejiang, China, dilution at 1:1000), Cyclic AMP-responsive element-binding protein 1 (CREB1, dilution at 1:6000; Proteintech, Wuhan, China), phospho-CREB1 (Ser133) (p-CREB1, dilution at 1:4000; Proteintech), protein kinase A (PKA, dilution at 1:10000; Proteintech), Activating Transcription Factor 1 (ATF1, dilution at 1:500; Proteintech), and anti-GAPDH (dilution at 1:10000; Proteintech). The secondary antibody was goat anti-rabbit IgG-HRP (Absin, Shanghai, China, dilution at 1:10000). Finally, the blot was visualized by enhanced chemiluminescence (ECL) kit (Proteintech).

Hematoxylin and eosin staining

Tissue was fixed using 4% paraformaldehyde and the slides were prepared after dehydration, transparent and wax immersion based on the protocol. Then, the slides were dewaxed hydrated using xylene and ethanol. After that, they were stained with hematoxylin for 2 min and eosin for 120 s. The slices were then dehydrated, transparent and sealed by ethanol, xylene and neutral resins, respectively. Finally, the sections were scanned and photographed using an Olympus BX53 microscope equipped with a 20x objective lens and images were captured with an Olympus DP27 digital camera.

Immunohistochemistry

The slides were prepared as described in H&E staining. After antigen retrieval, the sections were incubated with primary antibodies overnight at 4°C. For negative controls, the primary antibody was replaced with phosphate-buffered saline (PBS) or non-immune IgG. Human breast cancer tissue sections known to express GPER1 and Ki-67 were used as positive controls, respectively. Subsequently, the sections were incubated with HRP-conjugated goat anti-rabbit (ab150077, dilution at 1:200; Abcam, Cambridge, UK) for GPER1 or anti-mouse (ab150113, dilution at 1:200; Abcam) for Ki-67 secondary antibodies for 1 h at room temperature. The primary antibodies were anti-GPER1 (ab260033, dilution at 1:200; Abcam) and anti-Ki-67 (Maixin Biotechnology, Fujian, China; dilution at 1:300). After that, diaminobenzidine (DAB) chromogenic reagent was employed for color rendering.

The immunolabelling index for GPER1 and Ki-67 was estimated by assessing the percentage of positive cells. Five random microscopic fields per sample were captured at 200x magnification using a Olympus BX53 microscope. The number of positive cells and the total number of cells in each field were counted independently by two pathologists who were blinded to the group allocation. The immunolabelling index was calculated as (number of positive cells / total number of cells) × 100%. The average value from the five fields was used as the final score for each sample. All experiments were performed with six biological replicates (n=6). Finally, whole-slide images were acquired using an automatic scanning machine (Leica Aperio AT2) with a 20x objective lens.

CCK-8 assay

2×10^4 KYSE70 or KYSE150 cells were seeded into 96-well plates and cultured for 24 h. Then, 10 μL CCK-8 regent was added and incubated for 30 min at 37°C. Finally, the OD values at 450 nm were measured by a microplate reader (TECAN).

Flow cytometry assay for apoptosis

KYSE70 or KYSE150 cells in the logarithmic growth phase were collected by trypsinization without EDTA and washed twice with cold phosphate-buffered saline (PBS). The cells were then resuspended in 1X Binding Buffer at a density of 1×10^6 cells/mL. Subsequently, 100 μL of the cell suspension (approximately 1×10^5 cells) was transferred to a flow cytometry tube and stained with 5 μL of 7AAD-APC (Beyotime Biotechnology) for 10-15 min at room temperature in the dark, following the manufacturer's instructions. Immediately after staining, the samples were analyzed using a flow cytometer (BD Biosciences, Franklin Lakes, NJ, USA). For each sample, a minimum of 10,000 events were recorded. The apoptosis rate was defined as the percentage of 7AAD-positive cells in the analyzed population. All experiments were performed with three independent biological replicates, each with three technical replicates.

Transmission electron microscopy

The mitochondrial morphology in EC cells was assessed by transmission electron microscopy. Briefly, cells were collected and fixed with 2.5% glutaraldehyde in 0.1 M phosphate buffer (pH 7.4) at 4°C for at least 2 h. After washing with the same buffer, the cells were post-fixed with 1% osmium tetroxide in 0.1 M phosphate buffer for 1-2 h at room temperature. The samples were then dehydrated through a graded series of ethanol (30%, 50%, 70%, 80%, 90%, 95%, and 100%) for 15 min each, followed by two changes of pure acetone for 15 min each. Subsequently, the samples were infiltrated and embedded in SPI-PON 812 epoxy resin. Polymerization was conducted at 60°C for 48 h. Ultrathin sections (approximately 70 nm in thickness) were cut using an ultramicrotome (Leica UC7) and collected on copper grids. The sections were then double-stained with uranyl acetate (2% in 50% ethanol) for 15 min and lead citrate for 5 min to enhance contrast. Finally, the sections were observed, and images were acquired at a magnification of ×8,000 and ×12,000 using a transmission electron microscope (Hitachi HT-7800) operated at an accelerating voltage of 80 kV. At least 5 fields of view per sample were examined to assess the mitochondrial morphology.

Flow cytometry assay for ROS

KYSE70 or KYSE150 cells were seeded into 6-well plates at a density of 2×10^5 cells per well and cultured until they reached 70-80% confluency. According to the manufacturer's instructions, the

ROS assay reagent (Solarbio) was diluted 1:1000 in serum-free medium to prepare the working solution. The culture medium was then removed, and the cells were washed once with phosphate-buffered saline (PBS). Subsequently, 1 mL of the ROS working solution was added to each well, and the cells were incubated at 37°C in the dark for 30 min. After incubation, the cells were washed with PBS, harvested by trypsinization, and resuspended in 500 µL of PBS. The fluorescence intensity of the cells, which corresponds to the intracellular ROS levels, was immediately analyzed using a flow cytometer (BD Biosciences). For each sample, a minimum of 20,000 events were recorded. All experiments were performed with three independent biological replicates.

Measurement of Fe^{2+}

The level of Fe^{2+} in EC cells was detected by an iron assay kit (Solarbio) according to the manufacturer's instructions. Briefly, approximately 1×10^7 cells from each group were collected and washed with phosphate-buffered saline (PBS). The cells were then lysed and homogenized by ultrasonic wave in an ice bath. The supernatant was collected after centrifugation at 12,000 × g for 10 min at 4°C. Next, the chromogenic reagent was added to the supernatant and incubated at 25°C for 10 min. Finally, the OD values at 510 nm were measured using a microplate reader. All experiments were performed with three independent biological replicates.

Wound healing assay

Cells were incubated in a 24-well plate. After the cells covered the bottom of the well, draw a vertical line across the bottom of the well and measure the scratch width (0 h) using Image J software. After culturing for 24 h and 48 h, measured the scratch width again (24 h, 48 h) and calculate the cell migration rate [(0 h - 24 h) / 0 h × 100%].

Transwell assay

Cells from different group were resuspended, then added the cell suspension (2×105 cells) to the upper chamber of the Transwell (pre-coated with basement membrane matrix). Added serum-containing media to the lower chamber. After 24 h cultivate, fixed the cells, then with 0.5% crystal violet (Solarbio), the number of invading cells was counted under a microscope (Olympus, Tokyo, Japan).

ELISA

The level of cAMP was determined by cAMP Kit (Njjbio, Jiangsu, China). Briefly, 50 µL cell supernatant and 50 µL biotin antigen working solution were mixed and incubate at 37°C for 30 min. Next, 50µL avidin -HRP was added and incubated at 37°C for 30 min. After that, 50 µL chromogenic reagents A and 50µL chromogenic reagents B were added subsequently, and incubated at 37□ for 10 min. Next, 50 µL termination solution was added to terminate the reaction. Finally, the OD values at 450 nm were measured.

Bioinformatic analyses

The expression of GPER1 in EC and normal tissues and the prognostic value of GPER1 in EC patients in The Cancer Genome Atlas Program (TCGA) database were analyzed using the online tool Gene Expression Profiling Interactive Analysis (GEPIA) (http://gepia.cancer-pku.cn/). EC cells with or without GPER1 overexpression were collected and RNA-sequence was performed to compare the differential expressed genes (DEGs) between them. Kyoto Encyclopedia of Genes and Genomes (KEGG) enrichment analysis was performed based on these DEGs.

Pharmacological inhibition of cAMP/PKA pathway

To functionally validate the role of the cAMP pathway in GPER1-induced ferroptosis, KYSE70 and KYSE150 cells with or without GPER1 overexpression were treated with the cAMP/PKA pathway inhibitor H89 (MedChemExpress, Monmouth Junction, NJ, USA). Cells were divided into four groups: NC + Vehicle (DMSO), NC + H89 (10 µM), GPER1-OE + Vehicle (DMSO), and GPER1-OE + H89 (10 µM). The inhibitor or vehicle was added to the culture medium for 24 h prior to subsequent functional assays and molecular analyses.

Statistical analysis

GraphPad Prism 9 was applied for data analysis and plotting, and the results were showed as mean ±SD. Student's *t*-test was used to analyze the difference between two groups of data. Kaplan-Meier survival curve was employed to evaluate the prognostic value of GPER1 in EC patients.

Results

The expression of GPER1 reduced in EC

We analyzed the expression of GPER1 in EC and normal tissues using the TCGA database through GEPIA, and found that its level decreased in EC tissues (Figure 1a). Then, its value in predicting prognosis was explored *via* Kaplan-Meier curve which identified that high expression of GPER1 is positively correlated with the overall survival of EC patients (Figure 1b). After that, the levels of GPER1 mRNA in EC and esophageal epithelial cells were measured by qRT-PCR, and the results showed that the expression of GPER1 is lower in EC cells compared to HEEC (Figure 1c). Similarly, the abundance of GPER1 protein was not equal to that in HEEC (Figure 1d). Finally, IHC was employed to measure the level of GPER1 in EC and normal tissues, and the results were consistent with those of TCGA database (Figure 1e). The above results revealed the decreased expression of GPER1 in EC tissues.

Overexpression of GPER1 suppressed the cells migration and invasion *in vitro*

We also detected the effect of GPER1 overexpression on the migration and invasion of EC cells. As shown in Figure 2 a,b, we found that the migration rate of cells in the GPER1-OE group significantly decreased compared to the NC group (both $p<0.05$). Meanwhile, the invasion ability of cells also diminished in the GPER1-OE group significantly decreased compared to the NC group (both $p<0.05$). These results indicated that GPER1 overexpression could suppress cells migration and invasion.

Overexpression of GPER1 induces ferroptosis of EC cells

To investigate the role of GPER1 in EC, we employed lentiviral vectors to generate EC cells with stable overexpression of GPER1. The overexpression efficiency was validated using qRT-PCR and Western blotting (*Supplementary Figure S1 a,b*). We assessed cell proliferation using the CCK-8 assay and observed that increased GPER1 expression significantly reduced the proliferation capacity of both KYSE70 and KYE150 cell lines (Figure 3a). Furthermore, apoptosis levels were evaluated in these cell lines through flow cytometry analysis, revealing a higher proportion of apoptotic cells in the GPER1-overexpressing group compared to the NC group (Figure 3b, $p<0.05$). The cell morphology

of cells varies among ferroptosis, necrosis, apoptosis and autophagy. Thus, we firstly observed the morphology of organelles in EC cells to preliminary evaluate the possible causes leading to cell death. As shown in Figure 3c, the morphology of EC cells is mainly manifested by obvious mitochondrial contraction, increased membrane density and decreased or disappeared mitochondrial crest, which is in accord with ferroptosis.[9,10] Therefore, we hypothesized that overexpress GPER1 may induce ferroptosis of EC cells. To verify this, we firstly detected the ROS levels in EC cells and the data showed that more ROS generated when GPER1 expression increased in EC cells (Figure 4 a,b). Meanwhile, the content of Fe^{2+} in EC cells was measured, which was also increased in EC cells with increased GPER1 expression (Figure 4c). Finally, the expression of core markers of ferroptosis were detected, and the results displayed in Figure 4d revealed that enhanced GPER1 expression caused increased ASCL4 expression

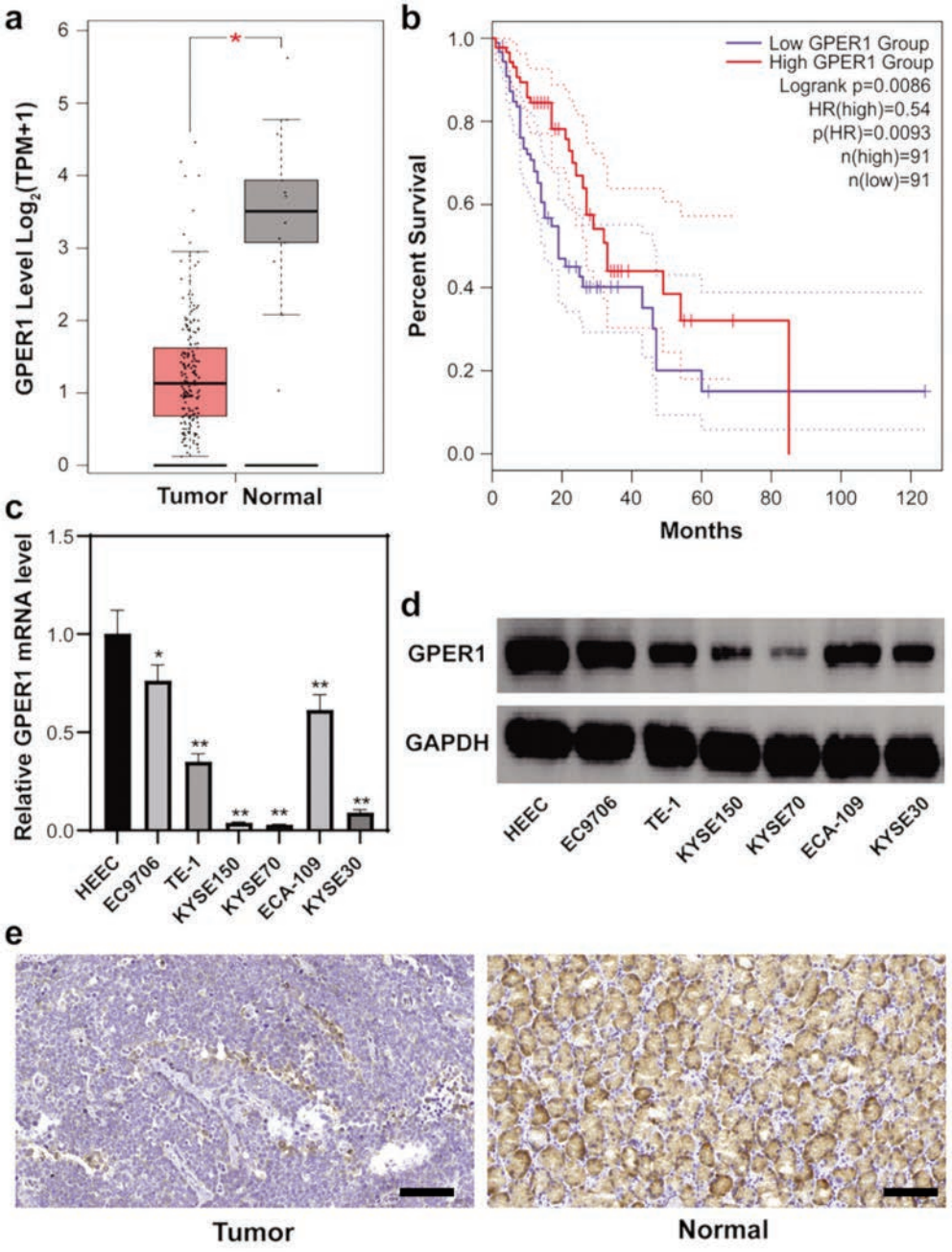

Figure 1. GPER1 expression reduced in EC. **a**) Expression of GPER1 in EC and normal tissues using the TCGA database. **b**) Kaplan-Meier survival curve of EC patients with GPER1 high and low expression in TCGA database. **c**) Levels of GPER1 in EC and normal esophageal epithelium cells detected by qRT-PCR. **d**) Levels of GPER1 in EC and normal esophageal epithelium cells detected by Western blotting. **e**) Representative figures displaying the expression of GPER1 in EC and normal tissues detected by immunohistochemistry; scale bar: 100 μm. Data are displayed as mean ± SD. Unpaired t-test, *p<0.05, **p<0.01.

in EC cells, while diminished GPX4. Furthermore, consistent results were observed when GPER1 was overexpressed in EC9706 cells, and opposite effects were achieved upon GPER1 knockdown in KYSE150 cells (*Supplementary Figure S2*), confirming the specific and bidirectional role of GPER1 in regulating ferroptosis. These results indicated that GPER1 overexpression leads to cell death was related to ferroptosis.

Overexpression of GPER1 causes tumor growth restriction *in vivo*

The influence of GPER1 on the progression of EC was further investigated *in vivo*. First, we confirmed the successful overexpression of GPER1 in the harvested tumor tissues by Western blotting (*Supplementary Figure S3*). Tumor volumes were measured on the 18th day following the subcutaneous injection of EC cells into nude mice. The disparity in tumor volumes between the two groups increased over time. Specifically, the growth rate of tumors in the NC group was significantly faster than that in the GPER1-OE group (Figure 5a). Subsequently, the mice were euthanized on day 32, and both tumor weight and volume were assessed. The findings indicated that both the weight and volume of tumors were reduced in the GPER1-OE group compared to the NC group (Figure 5 b,c). Additionally, IHC staining was performed to assess Ki-67 expression levels in tumors from both groups, revealing a

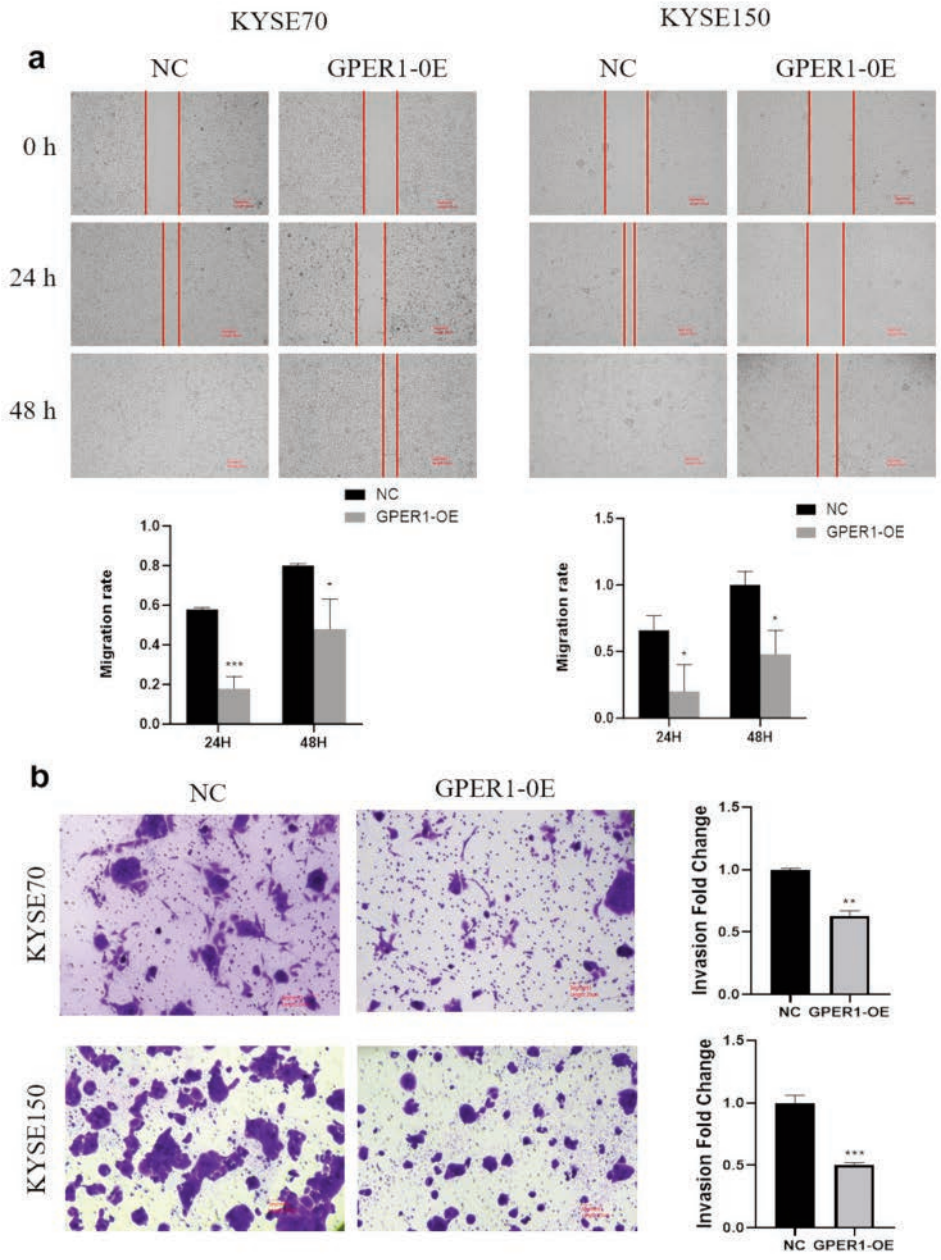

Figure 2. Overexpression of GPER1supresses cell migration and invasion. **a**) Migration of EC cells were detected by wound healing assay, and the statistical graph of migration rate was presented; scale bar: 50 μm. **b**) Invasion of EC cells were detected by Transwell assay, and the statistical graph of invasion ability was presented; scale bar: 20 μm. Unpaired t-test, *p<0.05, **p<0.01, ***p<0.001.

higher Ki-67 level in the NC group (Figure 5d). H&E staining showed that the tumor tissue in the NC group with disorganized cell arrangement. Cells exhibit significant pleomorphism, nuclear atypia, and scattered inflammatory cell infiltration. The GPER1-OE group displayed a relatively more uniform cellular population (Figure 5e). These results indicated that the overexpression of GPER1 results in the inhibition of EC growth *in vivo*.

Overexpression of GPER1 activates cAMP pathway in EC cells

To investigate the potential mechanism by which GPER1 promotes ferroptosis in EC cells, we initially constructed a protein-protein interaction (PPI) network to identify proteins that potentially interact with GPER1 (Figure 6a). Subsequently, KEGG enrichment analysis was conducted on these proteins, revealing the cAMP pathway as a potential downstream pathway regulated by GPER1 (Figure 6b). To validate the bioinformatics findings, we measured the cAMP content in the medium of EC cells and observed an elevated level of cAMP in the GPER1-overexpression (OE) group (Figure 6c). Furthermore, we assessed the expression of key proteins in the cAMP pathway and found increased levels of p-CREB1 (cAMP responsive element binding protein 1)/CREB1, PKA (protein kinase cAMP-activated catalytic subunit alpha), and ATF1 (activating transcription factor 1) in EC cells with GPER1 overexpression (Figure 6d). Collectively, these findings suggest that GPER1 may induce ferroptosis in EC cells by activating the cAMP pathway.

Inhibition of cAMP/PKA pathway reverses GPER1-induced ferroptosis

To determine whether the cAMP pathway is functionally required for GPER1-induced ferroptosis, we treated GPER1-overexpressing EC cells with the cAMP/PKA inhibitor H89. As shown in Figure 7 a,d, the decreased cell viability caused by GPER1 over-

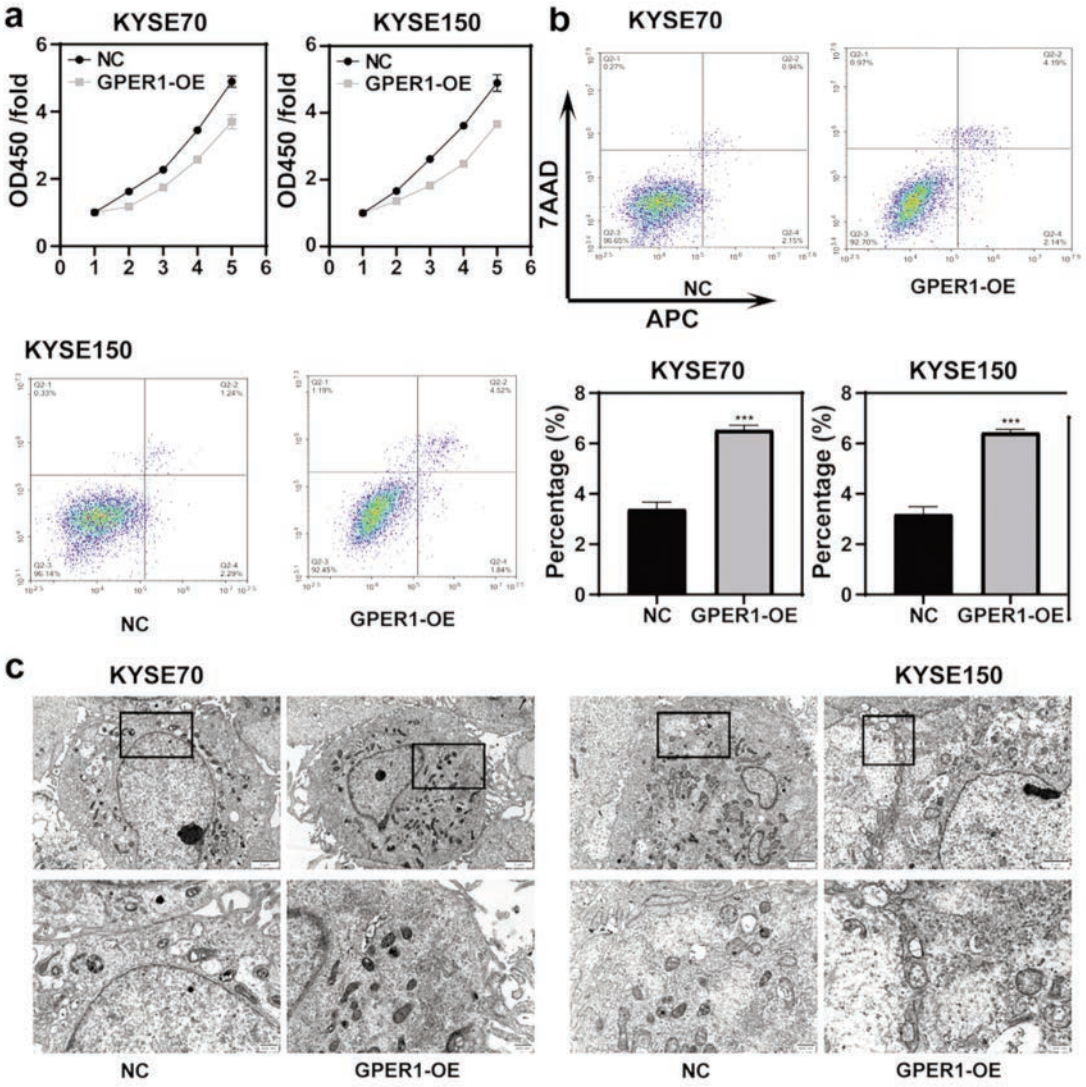

Figure 3. Overexpression of GPER1 promotes ferroptosis of EC cells *in vitro*. **a**) Proliferation ability of EC cells measured by CCK-8 assay. **b**) Cells apoptosis rate was detected by flow cytometry, and the statistical graph of the apoptosis of EC cells was measured. **c**) Representative figures of mitochondrial observed by TEM; scale bars: 2 μm.

expression was significantly rescued by H89 treatment. Accordingly, the elevated levels of ROS (Figure 7 b,e) and Fe^{2+} (Figure 7 c,f) in GPER1-OE cells were also markedly attenuated upon H89 incubation. At the molecular level, the overexpression of the pro-ferroptotic protein ACSL4 and the downregulation of the anti-ferroptotic protein GPX4 induced by GPER1 overexpression were reversed by H89 (Figure 7g). Furthermore, H89 treatment effectively suppressed the increased phosphorylation of CREB1 (p-CREB1) in GPER1-OE cells (Figure 7g), confirming the inhibition of the cAMP/PKA pathway. Collectively, these results demonstrate that pharmacological inhibition of the cAMP/PKA pathway alleviates GPER1-triggered ferroptosis, indicating that GPER1 promotes ferroptosis in EC cells primarily by activating the cAMP pathway.

Discussion

In this study, we assessed the expression levels and prognostic significance of GPER1 in EC tissues using data from TCGA *via* the GEPIA platform. Our analysis revealed a reduced expression of GPER1 in EC tissues, and higher GPER1 levels were associated with improved overall survival. Subsequently, we confirmed its expression in EC cell lines and fresh EC tissues, which also demonstrated a decreased expression of GPER1 in EC. Chou *et al*.[23] reported lower mRNA levels of GPER1 in papillary thyroid carcinoma samples compared to normal tissues, with low GPER1 expression correlating with extrathyroidal extension. Furthermore, Zhang *et al.* demonstrated higher expression of GPER1 correlated with a better clinical outcome in estrogen receptor-positive (ER+) breast cancer patients.[24] The trend of change in our analysis results is consistent with these two studies. Notably, the pro-ferroptotic effect of GPER1 was recapitulated in EC9706 cells, which have a higher basal GPER1 level, indicating that the function of GPER1 is not confined to cell lines with initial low expression.

The aberrant expression of GPER1 in EC suggests its potential involvement in progression of the disease. The role of GPER1 has been extensively investigated across various cancer types. Previous study demonstrated that GPER1 activation mitigates the progression of vulvar carcinoma cells, while its anti-tumor activity has also been confirmed in multiple myeloma.[25,26] Li *et al*. demonstrated that GPER-1 interacts with autocrine motility factor (AMF) and the complex contributes to endometrial cancer progression.[27] GPER1 also highly expressed in breast cancer cells.[28] Liu *et al.* indicated that the expression levels of GPER1 were higher in esophageal adenocarcinoma than in esophageal squamous cell carcinoma.[29] However, the role of GPER1 is not yet clear, and there is conflicting data. Especially, the specific function of GPER1 in EC remains unclear. Our findings revealed that the overexpression of GPER1 in EC cells inhibited tumor growth both *in vivo* and *in vitro*. Subsequent experiments suggested that elevated levels of GPER1 maybe facilitate ferroptosis in EC cells. It is specifically manifested in increasing the content of cellular ROS and Fe^{2+}, promoting the expression of ACSL4, and reducing the expression of GPX4. Currently, there are relatively few reports on the association between GPER1 and ferroptosis. Previously study demonstrated that GPER1 protected non-small cell lung cancer cells from ferroptosis.[30] Their results were opposite with our study. These differences not only reflect the complexity of ferroptosis regulation but also underscore the importance of tailored investigations into GPER1's role across distinct cancer types for potential therapeutic translation. We investigated the mechanism by which the overex-

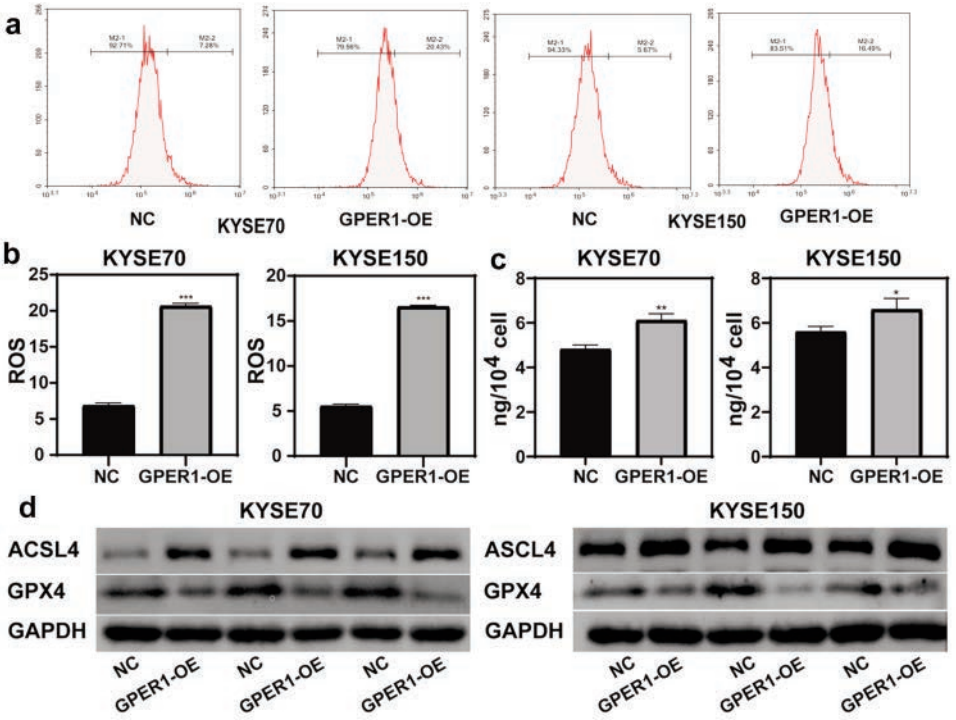

Figure 4. Overexpression of GPER1 induces ferroptosis of EC cells i*n vitro.* **a,b**) Statistical graph of ROS level in EC cells measured by flow cytometry. c) Level of Fe2+ in EC cells. d) Expression of GPX4 and ACSL4 in EC cells detected by Western blotting. Data are displayed as mean ±SD. Unpaired t-test, **p*<0.05, ***p*<0.01, ****p*<0.001.

pression of GPER1 inhibits EC tumor growth. KEGG enrichment analysis suggested that the cAMP signaling pathway may act as a downstream pathway of GPER1 in EC. As a second messenger, cAMP exerts pleiotropic effects on tumors. Its downstream effectors are diverse and include exchange protein activated by cAMP (EPAC), cAMP-dependent PKA, and ion channels. While cAMP can activate EPAC or PKA to promote cancer cell growth, it can also inhibit cell proliferation and survival in a context- and cancer type-dependent manner.[31] Additionally, cAMP has been identified as a regulator of ferroptosis in cancer cells.[32] Our experiments demonstrated that the levels of cAMP, p-CREB1/CREB1, PKA, and ATF1 increased following GPER1 overexpression in EC cells. Crucially, to establish a causal link, we employed a loss-of-function approach using the inhibitor H89. We found that blocking the cAMP/PKA pathway significantly reversed the ferroptotic phenotype induced by GPER1, including the restoration of cell viability, and the reduction of ROS, Fe^{2+}, and the pro-ferroptotic protein ACSL4. These functional data strongly suggest that the cAMP/PKA pathway is not merely associated with but is essential for mediating GPER1-induced ferroptosis in EC cells.

This study has several limitations. First, the sample size of human EC tissues in this study is a notable limitation. The investigation utilized only six paired EC tissue samples to assess the expression of GPER1. While this was sufficient to identify a significant downreg-

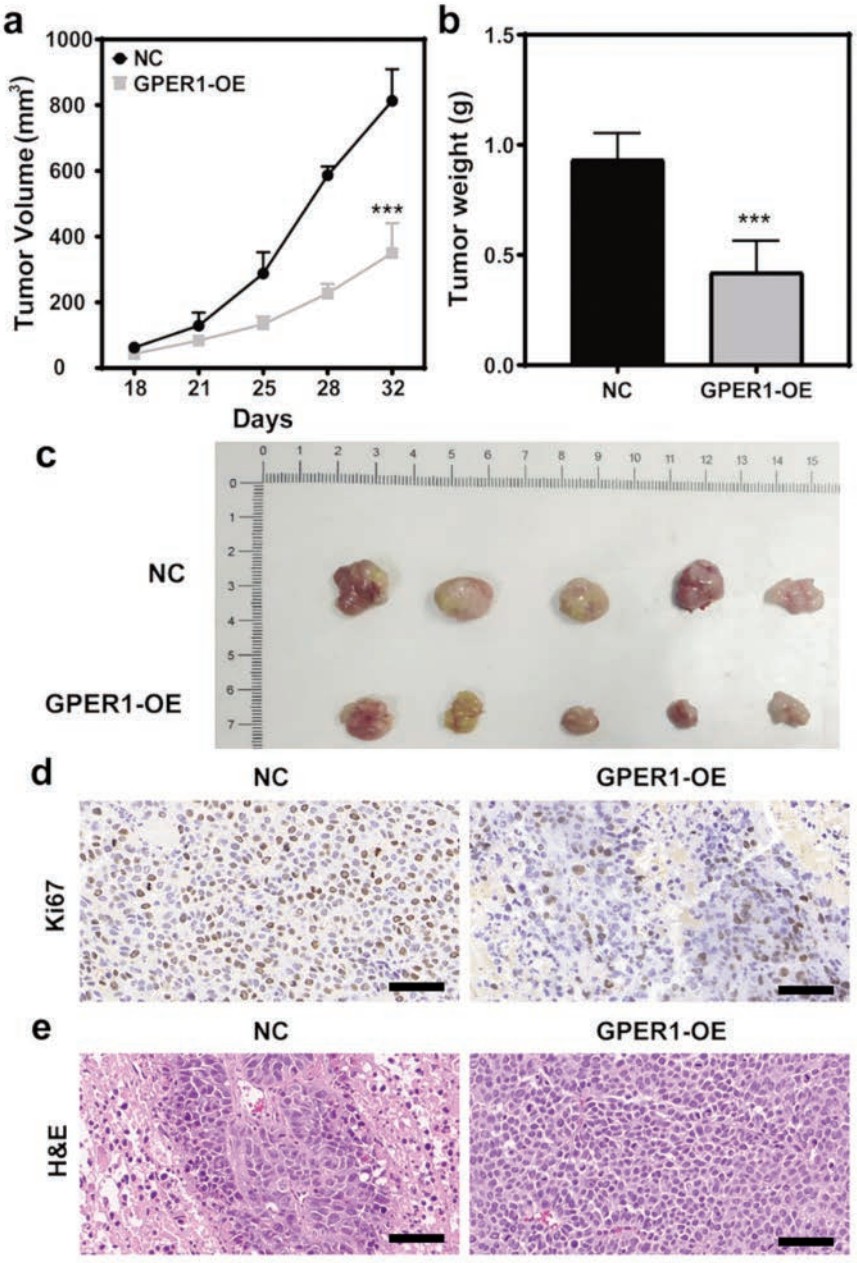

Figure 5. Overexpression of GPER1 causes growth restriction of EC *in vivo*. **a**) Volume of tumors measured from day 18 to 32. **b**) Weight of tumors measured at day 32. **c**) General view of tumors collected. **d**) Representative results of Ki-67 staining; scale bar: 100 μm. **e**) Representative results of H&E staining; scale bar: 100 μm. Data are displayed as mean ± SD. Unpaired t-test, ***p<0.001.

ulation of GPER1 in our cohort, this small sample size undeniably limits the statistical power and generalizability of our findings. A larger, independent cohort is required to validate the expression pattern and clinical relevance of GPER1 in EC. Furthermore, the limited sample size precluded us from performing robust subgroup analyses, such as correlating GPER1 expression with clinicopathological features (*e.g.*, tumor stage, metastasis) or patient survival, which represents an important area for future investigation. Lastly, although we have now functionally validated that the cAMP pathway serves as a critical mediator between GPER1 and ferroptosis, it remains to be determined whether other downstream effectors also contribute to this process. Despite the aforementioned limitations, it can be concluded that GPER1 expression is reduced in EC tissues. Furthermore, the overexpression of GPER1 appears to enhance ferroptosis in EC, with the cAMP pathway potentially serving as the primary link between GPER1 and ferroptosis in this context.

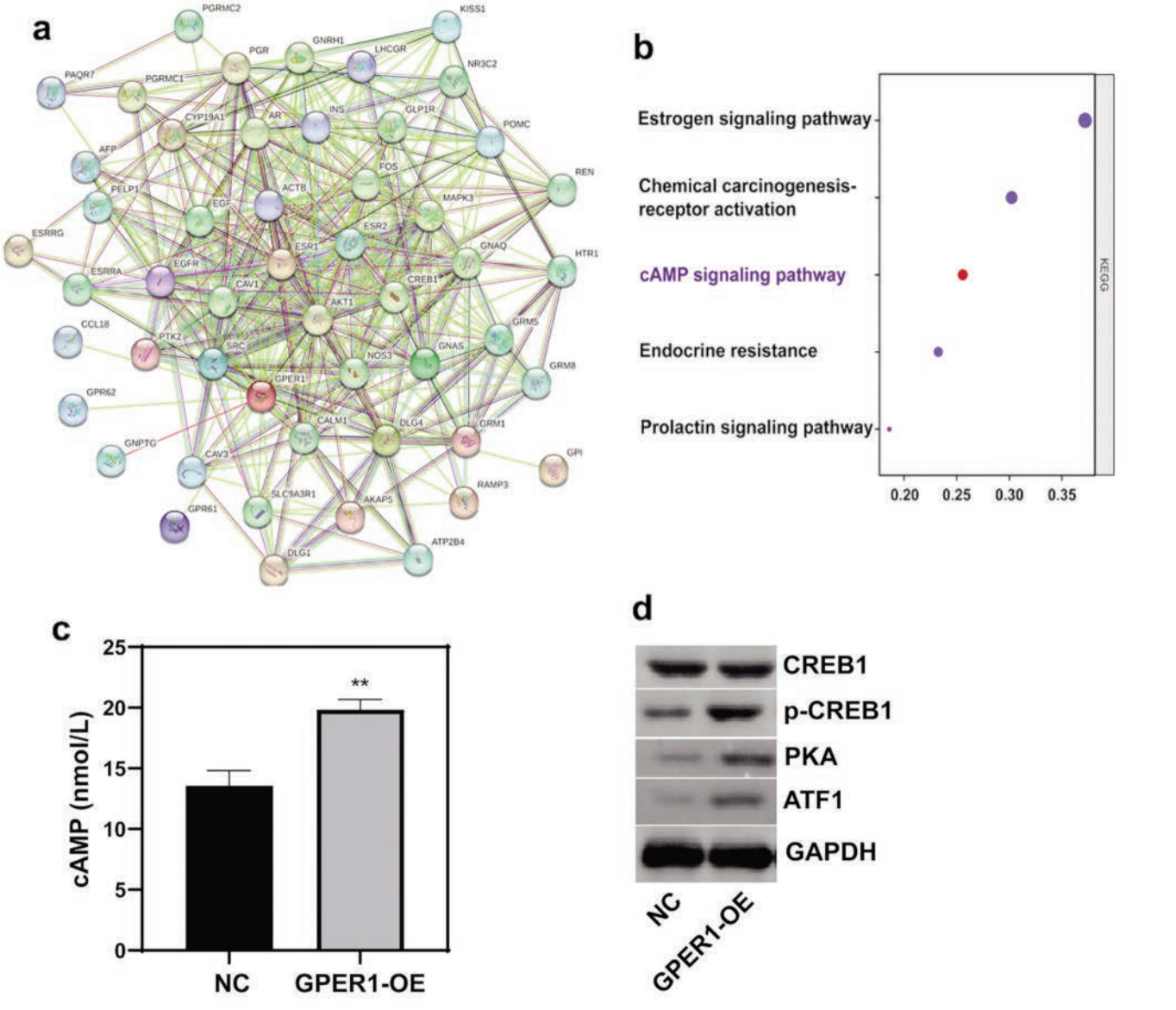

Figure 6. Overexpression of GPER1 activates cAMP pathway in EC cells. **a**) Protein-protein interaction (PPI) network analysis of GPER1-interacting proteins. **b**) KEGG enrichment analysis of differential expressed genes. **c**) Level of cAMP detected by ELISA. **d**) Expression of p-CREB1, CREB1, PKA and ATF1 in EC cells detected by Western blotting. Data are displayed as mean ± SD. Unpaired t-test, $^{**}p<0.01$.

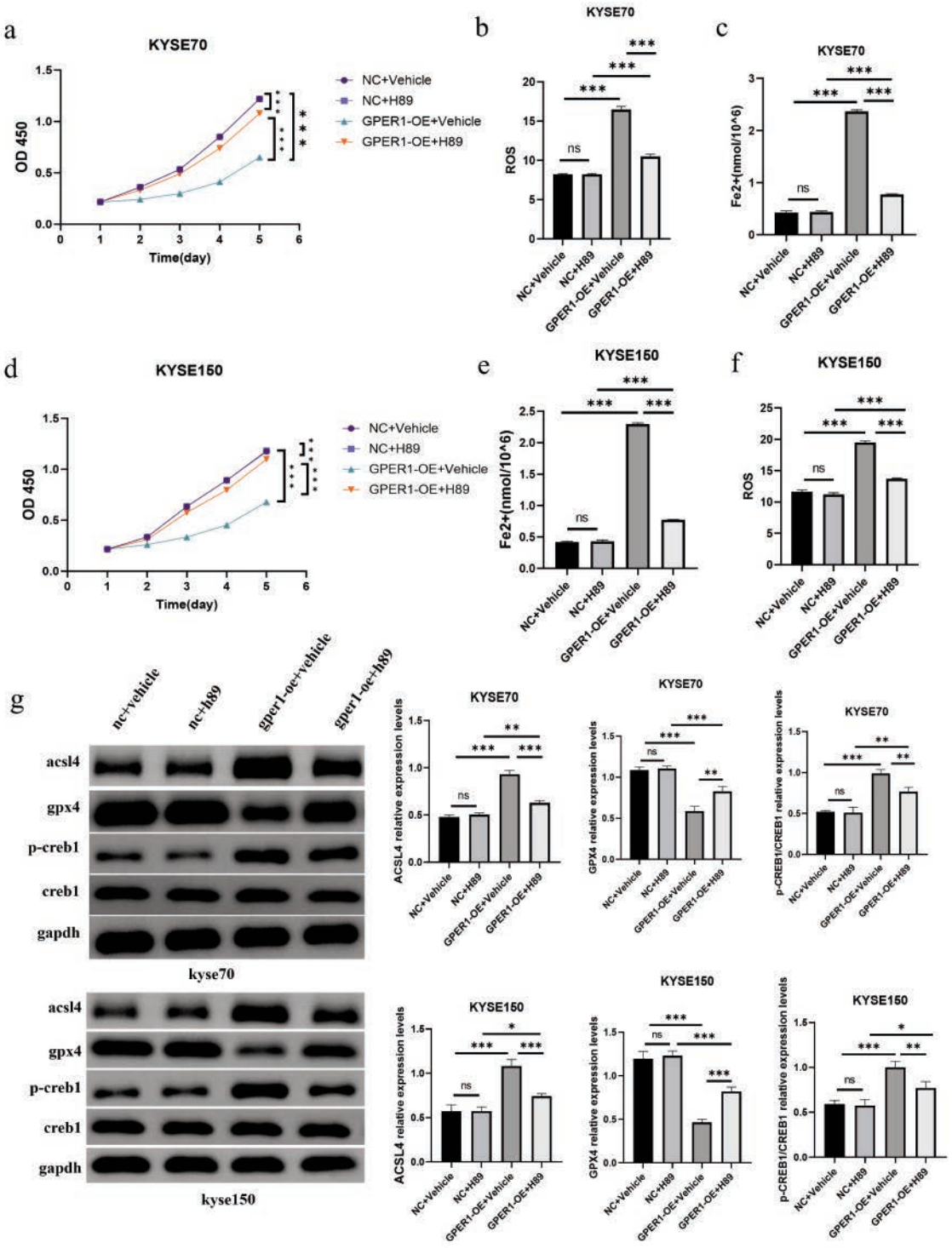

Figure 7. Inhibition of the cAMP/PKA pathway attenuates GPER1-induced ferroptosis in esophageal cancer cells. KYSE70 and KYSE150 cells were treated with or without the cAMP/PKA inhibitor H89 (10 μM) for 24 h under four conditions: negative control with vehicle (NC + Veh), negative control with H89 (NC + H89), GPER1 overexpression with vehicle (GPER1-OE + Veh), and GPER1 overexpression with H89 (GPER1-OE + H89). **a,d**) Cell viability was determined by CCK-8 assay in KYSE70 (**a**) and KYSE150 (**d**) cells. **b,e**) Intracellular ROS levels were measured by flow cytometry using a DCFH-DA probe in KYSE70 (**b**) and KYSE150 (**e**) cells. **c,f**) Intracellular Fe^{2+} content was quantified by an iron assay kit in KYSE70 (**c**) and KYSE150 (**f**) cells. **g**) Protein expression levels of the ferroptosis markers ACSL4 and GPX4, and the cAMP pathway components p-CREB1 and CREB1, were analyzed by Western blotting in both KYSE70 and KYSE150 cells; left panels show representative Western blot images, and the right panels show the corresponding quantitative densitometric analysis of the protein bands, normalized to GAPDH (for ACSL4 and GPX4) or total CREB1 (for p-CREB1). All quantitative data are presented as the mean ±SD from three independent experiments (n=3). Statistical significance was determined by one-way ANOVA followed by Tukey's post-hoc test; *p<0.05, **p<0.01, ***p<0.001, ****p<0.0001; ns, not significant.

References

1. Ferlay J, Soerjomataram I, Dikshit R, Eser S, Mathers C, Rebelo M, et al. Cancer incidence and mortality worldwide: sources, methods and major patterns in GLOBOCAN 2012. Int J Cancer 2015;136:E359-86.
2. Pennathur A, Gibson MK, Jobe BA, Luketich JD. Oesophageal carcinoma. Lancet 2013;381:400-12.
3. Fokas E, Schlenska-Lange A, Polat B, Klautke G, Grabenbauer GG, Fietkau R, et al. Chemoradiotherapy plus induction or consolidation chemotherapy as total neoadjuvant therapy for patients with locally advanced rectal cancer: long-term results of the CAO/ARO/AIO-12 randomized clinical trial. JAMA Oncol 2022;8:e215445.
4. Polednak AP. Trends in survival for both histologic types of esophageal cancer in US surveillance, epidemiology and end results areas. Int J Cancer 2003;105:98-100.
5. Christie NA, Patel AN, Landreneau RJ. Esophageal palliation--photodynamic therapy/stents/brachytherapy. Surg Clin North Am.2005;85:569-82.
6. van Rossum PSN, Mohammad NH, Vleggaar FP, van Hillegersberg R. Treatment for unresectable or metastatic oesophageal cancer: current evidence and trends. Nat Rev Gastroenterol Hepatol 2018;15:235-49.
7. Dixon SJ, Lemberg KM, Lamprecht MR, Skouta R, Zaitsev EM, Gleason CE, et al. Ferroptosis: an iron-dependent form of non-apoptotic cell death. Cell 2012;149:1060-72.
8. Yang WS, SriRamaratnam R, Welsch ME, Shimada K, Skouta R, Viswanathan VS, et al. Regulation of ferroptotic cancer cell death by GPX4. Cell 2014;156:317-31.
9. Xie Y, Hou W, Song X, Yu Y, Huang J, Sun X, et al. Ferroptosis: process and function. Cell Death Differ 2016;23:369-79.
10. Stockwell BR, Friedmann Angeli JP, Bayir H, Bush AI, Conrad M, Dixon SJ, et al. Ferroptosis: a regulated cell death nexus linking metabolism, redox biology, and disease. Cell 2017;171:273-85.
11. Lei G, Zhuang L, Gan B. Targeting ferroptosis as a vulnerability in cancer. Nat Rev Cancer 2022;22:381-96.
12. Liang C, Zhang X, Yang M, Dong X. Recent progress in ferroptosis inducers for cancer therapy. Adv Mater 2019;31:e1904197.
13. Masi M, Racchi M, Travelli C, Corsini E, Buoso E. Molecular characterization of membrane steroid receptors in hormone-sensitive cancers. Cells 2021;10:2999.
14. Filardo EJ, Thomas P. Minireview: G protein-coupled estrogen receptor-1, GPER-1: its mechanism of action and role in female reproductive cancer, renal and vascular physiology. Endocrinology 2012;153:2953-62.
15. Fuentes N, Silveyra P. Estrogen receptor signaling mechanisms. Adv Protein Chem Struct Biol 2019;116:135-70.
16. Gaudet HM, Cheng SB, Christensen EM, Filardo EJ. The G-protein coupled estrogen receptor, GPER: The inside and inside-out story. Mol Cell Endocrinol 2015;418 Pt 3:207-19.
17. Revankar CM, Cimino DF, Sklar LA, Arterburn JB, Prossnitz ER. A transmembrane intracellular estrogen receptor mediates rapid cell signaling. Science 2005;307:1625-30.
18. Tian S, Zhan N, Li R, Dong W. Downregulation of G protein-coupled estrogen receptor (GPER) is associated with reduced prognosis in patients with gastric cancer. Med Sci Monit 2019;25:3115-26.
19. Han N, Heublein S, Jeschke U, Kuhn C, Hester A, Czogalla B, et al. The G-protein-coupled estrogen receptor (GPER) regulates trimethylation of histone H3 at lysine 4 and represses migration and proliferation of ovarian cancer cells in vitro. Cells 2021;10:619.
20. Qiu YA, Xiong J, Fu Q, Dong Y, Liu M, Peng M, et al. GPER-induced ERK signaling decreases cell viability of hepatocellular carcinoma. Front Oncol 2021;11:638171.
21. Yang Y, Sheng J, Hu S, Cui Y, Xiao J, Yu W, et al. Estrogen and G protein-coupled estrogen receptor accelerate the progression of benign prostatic hyperplasia by inducing prostatic fibrosis. Cell Death Dis 2022;13:533.
22. Xu T, Ma D, Chen S, Tang R, Yang J, Meng C, et al. High GPER expression in triple-negative breast cancer is linked to pro-metastatic pathways and predicts poor patient outcomes. NPJ Breast Cancer 2022;8:100.
23. Chou CK, Chi SY, Hung YY, Yang YC, Fu HC, Wang JH, et al. Decreased expression of estrogen receptors is associated with tumorigenesis in papillary thyroid carcinoma. Int J Mol Sci 2022;23:1015.
24. Zhang N, Sun P, Xu Y, Li H, Liu H, Wang L, et al. The GPER1/SPOP axis mediates ubiquitination-dependent degradation of ERα to inhibit the growth of breast cancer induced by oestrogen. Cancer Lett 2021;498:54-69.
25. Loris J, Hanesch L, Bauerschmitz G, Gallwas J, Gründker C. Activation of G-protein-coupled estrogen receptor 1 (GPER1) reduces progression of vulvar carcinoma cells. Int J Mol Sci 2023;24:13705.
26. Gallo Cantafio ME, Torcasio R, Scionti F, Mesuraca M, Ronchetti D, Pistoni M, et al. GPER1 activation exerts anti-tumor activity in multiple myeloma. Cells 2023;12:2226.
27. Li Y, Jia Y, Bian Y, Tong H, Qu J, Wang K, et al. Autocrine motility factor promotes endometrial cancer progression by targeting GPER-1. Cell Commun Signal 2019;17:22.
28. Kalabay M, Szász Z, Láng O, Lajkó E, Pállinger É, Duró C, et al. Investigation of the antitumor effects of tamoxifen and its ferrocene-linked derivatives on pancreatic and breast cancer cell lines. Pharmaceuticals (Basel) 2022;15:314.
29. Liu J, Niu Y, Zhang B, Sun Q, Li H, Bai L, et al. Different expression pattern of G protein-coupled estrogen receptor GPER1 in esophageal squamous cell carcinoma and adenocarcinoma. Int J Mol Sci 2023;24:14055.
30. Chen J, Zhao R, Wang Y, Xiao H, Lin W, Diao M, et al. G protein-coupled estrogen receptor activates PI3K/AKT/mTOR signaling to suppress ferroptosis via SREBP1/SCD1-mediated lipogenesis. Mol Med 2024;30:28.
31. Zhang H, Liu Y, Liu J, Chen J, Wang J, Hua H, et al. cAMP-PKA/EPAC signaling and cancer: the interplay in tumor microenvironment. J Hematol Oncol 2024;17:5.
32. Tang H, Kang R, Liu J, Tang D. ATF4 in cellular stress, ferroptosis, and cancer. Arch Toxicol 2024;98:1025-41.

Online Supplementary Material

Figure S1. Efficiency of GPER1 over-expression in EC cells detected by qRT-PCR.

Figure S2. Modulation of GPER1 expression bidirectionally regulates ferroptosis in EC cells.

Figure S3. Stable overexpression of GPER1 in tumor tissues at the endpoint of the in vivo study.

Received: 23 September 2025. Accepted: 2 December 2025.

European Journal of Histochemistry 2026; 70:4422
doi:10.4081/ejh.2026.4422